STATE RESEARCH CENTER OF RUSSIA

INSTITUTE FOR HIGH ENERGY PHYSICS

V.Ammosov, A.Ivanilov, V.Koreshev, Yu.Sviridov[*], V.Zaets

State Research Centre of Russian Federation
Institute for High Energy Physics
142284 Protvino, Moscow region, Russia

A.Semak

Moscow Engineering and Physics Institute
Moscow, Russia

MULTI-STRIP READ-OUT IN RPCS: CROSS-TALKS AND CLUSTER SIZE

[*] Corresponding author, E-mail: yu_sviridov@mx.ihep.su

Protvino 1999

Abstract

Ammosov V., Ivanilov A., Koreshev V., Semak A., Sviridov Yu., Zaets V. Multi-Strip Read-Out in RPCs: Cross-Talks and Cluster Size.: IHEP Preprint 99–52. – Protvino, 1999. – p. 19, figs. 13, refs.: 14.

Study of cross talks and their correlation with an observed cluster size for multi-strip RPC read-out was carried out using the beam and Inner Spark Pulser data. The marked influence of the surface resistivity of the HV electrode graphite coating on the induced charge spread among the read–out strips was observed. The waveforms and relative amplitudes of the CT signals were studied for different discharge positions across the strips. No cross talks and cluster size reduction was obtained for the strip panel with tiny screening strips as compared with the ordinary panel.

Аннотация

Аммосов В.В., Иванилов А.А., Корешев В.И., Свиридов Ю.М., Семак А.А., Заец В.Г. Многостриповое считывание в РПК: перекрестные наводки и размер кластера.: Препринт ИФВЭ 99–52. – Протвино, 1999. – 19 с., 13 рис., библиогр.: 14.

Проведено изучение перекрестных наводок (ПН) и их корреляции с размером кластера при многостриповом считывании сигналов Резистивных Плоских Камер. Данные получены методом внутреннего искрового разрядника, а также на пучке частиц. Наблюдалось существенное влияние поверхностного сопротивления графитового покрытия высоковольтного электрода на растекание индуцированного заряда по поверхности считывающей стриповой панели. Изучены форма и относительная амплитуда сигналов ПН в зависимости от положения лавины/стримера относительно границ стрипа. Не обнаружено подавления ПН и размеров кластера для панели с узкими экранирующими стрипами по сравнению с обычной панелью.

INTRODUCTION

In the ATLAS experiment, the proposed Resistive Plate Chambers (RPCs) consist [1] of the gas gap enclosed by two resistive (bakelite) electrodes. High voltage is supplied to the outer surfaces of bakelite plates using graphite paint with the surface resistivity of the order of 100 kΩ/square. Electrons produced in the gas gap develop discharge in the high uniform electric field inside the gap. The discharge induces a signal in the read-out electrodes placed on both sides of the gas gap. These electrodes are made as strips arranged in the X direction in one strip panel and in the Y direction — in the opposite panel. Strip width of about 30 mm is determined by both physical demands and the cost of the required electronics. Signals produced on the strips are amplified, discriminated, shaped and used further in the trigger logic.

One of the main characteristics of the RPCs as muon trigger detectors is the number of strips fired per one through going particle (cluster size). Large cluster size worsens the accuracy of the particle track localization and is undesirable in the detectors working in a digital "yes/no" read-out mode.

The sources of the multiple firing of several read-out channels are the processes usually called "the cross talks" (CT). The CT phenomenon is habitual for different "open" multichannel systems [2]. Various sources of the CTs can exist in particular systems [3]. First and the most fundamental one is the induction effect that is responsible for the creation of a useful signal but also for the unwanted pulses on surrounding electrodes [4–8]. The others are connected with different parasitic couplings between electrodes [3,9].

The CTs in RPC and related detectors were considered by some groups [10-13]. A general conclusion can be made from the published data that these characteristics are very special ones for each particular detector design.

Beard et al. [10] studied the cross talks for the pad read-out in a thin gap MWPC. The pad dimensions were roughly $18{\times}23$ cm^2. The authors identified and disentangled three sources of cross talks in terms of capacitive couplings between (a) adjacent pads, (b) pads and anode wires, and (c) pads and a resistive cathode.

Mari et al. [11] performed a systematic study of CTs in a 2 mm gap glass RPC of the design analogous to the ATLAS RPC. Pick-up strips (10 mm wide) were faced to the cathode, and the opposite pick-up electrode was made as a pad $15{\times}15$ cm^2. The authors varied distances between the cathode and related pick-up strips and between the anode and pick-up pad. For the standard set-up, the distance between opposite conducting planes was equal to 6.1 mm. Unipolar signals were observed for strips i=±1 and ±2, where i=0 refer to the triggered strip. These signals

had the triggered strip polarity for both (0.2 mm and 4 mm) positions of the pick-up strips relative to the cathode plane, but they were inverted for the case where the opposite pick-up pad was shifted by 4 mm from the anode plane. The authors developed a program capable of reproducing all the features observed.

Crotty et al. [12] detected signals on adjacent strips in the 8 mm wide gap RPC. Strip width was 12.5 mm on 15 mm pitch. High voltage (+ or −) was applied to the gas gap by the cooper electrode on one side of the gap, and pick-up strips were placed to the other side. The distance between conducting planes in the set-up was equal to about 10.5 mm. The authors detected unipolar pulses on the strip adjacent to the triggered one for both positive and negative voltage on the HV electrode. But if for the positive potential on the HV electrode (that is, the strips facing the cathode) the CT pulses had the same polarity as the triggered strip signals, for the negative polarity these signals were "often" [12] inverted.

In the present paper some results of the CTs and cluster size studies in the 2 mm gap bakelite RPC are presented. These results were obtained both using the Inner Spark Pulser (ISP) method [9] and during the beam exposures of the chamber. The goals of this study were:

— to obtain quantitative data on CTs in the RPC design similar in the main to the ATLAS proposal;
— to estimate a correlation between CTs values and cluster size, and
— to investigate the nature of CTs.

The paper is organized as follows. In Section 1 the experimental methodic is briefly described. In Section 2, the results on CTs are presented. Section 3 contains some data about cluster size measurements. In Section 4 some CT results are presented that are of more general interest. In Section 5 we discuss the obtained results and the last section contains our conclusion.

1. EXPERIMENTAL APPARATUS

The RPC used for beam studies had one 2.1 mm wide gas gap with lateral dimensions 0.5×2 m^2. The HV electrodes were made from 1.6 mm thick phenol-melamine plates having $(1\text{-}3)\times10^{12}$ Ωcm volume resistivity. The bakelite plates were glued together through PVC frames and spacers. The applied voltage was spread over the outer electrodes surfaces by graphite paint. No additional treatment was applied to the inner surfaces of the gas gap.

The chamber had X and Y read-out strip panels. The results presented refer to the 2 m long X-strips (16 in total). Two designs of this X-panel were studied. In both of them strips were scratched on the copper laminated G10 sheets 0.5 mm thick; a similar sheet was used for the return electrodes of the panels. These sheets were glued onto the 2 mm thick foam plate to obtain 3 mm thick panels. The first panel studied ("ordinary" panel) was the simplest panel with the sensitive strips 28 mm wide and 2 mm gaps between them. In the second panel ("screened" panel) the screening tiny strips 1 mm wide were made between the sensitive strips. These screening strips were terminated with resistors equal to their measured impedance of 130 Ω. The impedances of the sensitive strips were equal to 24 Ω. These strips were terminated on both ends with 50 Ω resistors to match, together with the input impedance of the amplifiers, the impedance of the strip line.

The beam data were obtained on the test beam of U–70 IHEP accelerator. The trigger was worked out by fourfold coincidence of scintillation counters S1–S4 (Fig. 1–a) and picked out

1.5×4 cm^2 area of one vertical X-strip (further on — the "reference" strip). Veto-counter with 25 mm diameter hole in front of the RPC was added to the trigger in some exposures.

Long strips under study were connected at one end (Fig. 1–b) to 16–channels amplifier/discriminator ATL161 with two thresholds of 0.5 and 1.0 mV. Outputs of ATL161 were fed to the TDC with about 0.7 ns binning. TDC gates were 400 and 500 ns. TDC data were used for cluster size measurements.

Opposite ends of strips were used for waveform observation and relative amplitude measurements on different strips using digital oscilloscope with 500 MHz bandwidth and 2 Gs/s sampling rate. A reference strip was also used for the efficiency, singles rate and reference charge measurements. The QDC used had sensitivity of 0.26 pC/count. The QDC gate width was varied from 100 to 500 ns.

We used mixtures of $C_2H_2F_4/iC_4H_{10}/SF_6$ in the following flow rate compositions: 97/3/0, 96.5/3/0.5, 96/3/1, 95/3/2, 92/3/5 and 98/0/2.

The ISP is essentially a needle under high potential inserted into the gas gap. In our design, the ISP was made as a section of gas gap mock-up (Fig. 2–a); the needle of the ISP was put (Fig. 2–b) through the upper bakelite plate. A remaining gap between the needle and the lower plate was about 0.4 mm. Just under the needle a thin cooper foil was glued to the lower bakelite to form about 50 mm^2 conducting spot to stabilize the ISP operation. HV was fed to the needle by the graphite coating. The whole set-up included the ISP, strip panels and the gas gap mock-up. The gas gap mock-up was made as a set of 10, 35, 50 and 100 cm long sections to form, including ISP, the 2 m long unit (Fig. 2–a). The ISP was made 5 cm wide in a strip direction and 70 cm long in a perpendicular direction, to provide a possibility of moving spark position across the strip.

The principle of ISP operation is simple: For some threshold voltage applied to the needle, sparks appear in the gap between the needle tip and the lower bakelite plate. Sparking frequency increases linearly with applied voltage and is some tens Hz. The amplitude of the pulse on strip just under the needle (reference strip) was a few volts and was stable to at least 10%. The signals on the reference and neighbour strips were observed and measured with a usual oscilloscope.

We studied with the ISP the two above mentioned strip panels and additionally 55 cm long panel. One half of this panel was similar in design to the "ordinary" panel and the other — to the "screened" panel, thus providing the possibility of direct comparison of the screening strips effects. The screening strips of this panel were grounded on both ends.

During the beam exposure, the positive voltage was applied to the chamber and the long strips under study were those close to the anode. The performance of the RPC with respect to efficiency, HV plateau width, charge properties and other characteristics are described elsewhere [13]. In the ISP studies, both positive and negative polarities were applied to the needle.

2. CROSS TALKS STUDY

Important information about the nature of CTs can be obtained from the observation of the waveforms of voltage signals on different strips.

On Fig. 3 the typical waveforms of signals are shown for the reference strip (i=0) and for strips i=±1 and i=±2. These signals were observed with a digital oscilloscope during the beam exposure and for the "ordinary" panel. The RPC was operated with a binary 97/3/0 gas mixture at the HV set 400 V above the plateau knee. The trigger was modified to pick-out narrower region of the detector plane, 0.3(across strip)×4(along strip) cm^2. The results presented were

obtained for the trigger position on the axis of the reference strip. Signals from i=±1, ±2 strips were amplified by 20 and those of the reference strip by 4 (Fig. 3–a, b, c, d) or 7 (Fig. 3–e, f, g, h).

Fig. 3–a, b, c and d refer to the case of low — about 50 kΩ/sq — graphite resistivity and Fig. 3–e, f, g, h — to the high — 500 kΩ/sq — resistivity. For the low resistivity anode, the long tails of the opposite polarity are seen for the reference signals. The amplitudes of these tails are about (10–15)% of the useful signals. The corresponding long pulses appear on the neighbour strips superimposed on the prompt CT signals. These long pulses have the polarity of the reference signals. In [8] such an effect was predicted by simulation and was attributed to the discharging of "reference strip–graphite" effective capacitance C^*, that was charged by avalanche/streamer development in the gas gap, through graphite effective resistance R^*. The amplitudes of these long pulses should be roughly R_S/R^* of the signal on a reference strip, where R_S is the strip load. Thus, for the higher resistivity anode such effect is strongly suppressed.

The difference seen on Fig. 3–a and 3–c in signal waveforms for strips i=+1 and i=−1 was caused most likely by the trigger offset from the reference strip axis. It should be stressed (Fig. 3–c, d) that the amplitudes of the long parasitic pulses are often higher than those of the fast CT signals.

The fast CT signals (Fig. 3–e, f, g, h) have a distinguished bipolar shape. For the strips i=±1 the CT signal has a bipolar shape with the leading pulse of the reference polarity. It looks like a derivative of the reference negative signal on strip i=0.

For all other strips, the CT signals are also bipolar but "inverted", with positive leading pulses.

Similar waveforms were also observed with the ISP for all the above-mentioned panels and for the needle position on the reference strip axis. Also these features do not depend on the polarity of the HV applied to the needle of ISP except, certainly, for simultaneous inverting of all the pulses.

The number of strips fired when a particle traverses the gas gap (cluster size) depends on the amplitudes of signals induced on different strips.

The distribution of relative amplitudes r_{i0} between strips for the trigger position near the reference strip axis were obtained with a digital oscilloscope and are shown on Fig. 4 for the "ordinary" panel and two graphite resistivities. We have defined the relative CT amplitudes r_{i0} as

$$r_{i0} = A_i/A_0, \tag{1}$$

where A_i, A_0 are the amplitudes of signals on strip "i" and the reference strip (i=0), respectively. For bipolar signals, only the pulses of reference polarity were considered. For the low resistivity, two data sets are shown, for the direct fast CT signals and for the long parasitic ones.

For a high resistivity case and for prompt signals in a low resistivity case, the relative CT amplitudes for i=±1 strips are equal to 0.05, about 0.006 — for i=±2 strips and only 0.002–0.003 for the other strips.

The indication is seen that for long pulses in the case of low resistivity anode, the distribution is wider: r_{10} is about 0.1, $r_{20} \simeq 0.03$ and for other strips r_{i0} seem to be not lower than 0.01.

The CT study with the ISP provided us with a first possibility (confirmed by the beam data, see later) to observe the waveform and relative amplitudes gradual changing in dependence of the discharge position across the strip. It was found in particular that the reference signal retains its shape for the needle position up to the distance of about 18 mm from the strip axis (that is, 4 mm outside the reference strip edge and 2 mm inside the adjacent strip region) and only then changes it to the one shown on Fig. 3–e, f for i=±1. The similar behaviour was observed

4

for the adjacent strip: Bipolar shape transforms to the unipolar one for the needle position still inside the reference strip. In other words, both neighbour strips have identical signal waveforms for the "edge region" of about $\pm$(3–4) mm near the midline between these strips.

On Fig. 5 the ratio r_{10} is shown in dependence of the ISP needle position across the strips i=0 and i=+1. Superimposed on this figure are also the beam data ("ordinary" panel, low graphite resistivity, only fast CT signals of the reference polarity were considered) showing the ratios r_{10} and r_{20} as a function of trigger position. A general agreement is seen. The $r_{10}(r_{20})$ ratios vary from 0.05(0.006) at the reference strip axis to 1(0.06) — for the needle position between two adjacent strips, respectively.

A short run was carried out with the negative HV applied to the chamber that is the long read-out strips facing the cathode. No differences in the CT signal waveforms were observed except the obvious inversion. Some results regarding the CT distribution between strips in this case are shown on Fig. 5. It seems that these characteristics are similar for both "anode" and "cathode" strips.

The effect of the screening strips was studied with ISP both on the two 2 m long panels used during the beam tests and on the 55 cm long combined strip panel described above, to exclude possible systematics. The results are presented on Fig. 6. On Fig. 6–a signal partition between adjacent strips i=0 and i=1 for different needle positions with respect to strips is shown for both "screened" and "ordinary" long panels. There is not seen a pronounced difference between two data sets. On Fig. 6–b, the possible effect of screening strips is shown in terms of screening coefficient R_i defined as

$$R_i = (r_{i0})_{SC}/(r_{i0})_{ORD}. \tag{2}$$

Here the subscripts SC(ORD) refer to screened(ordinary) parts of the short panel, respectively. In these measurements the ISP needle was positioned above the reference strip axis. No significant reduction in CTs relative amplitudes is seen for the "screened" panel with respect to the "ordinary" one.

3. CLUSTER SIZE STUDY

For the given CT signals distribution among the strips, the cluster size depends on the charge produced in the discharge process and on the discriminator threshold. The dependence of the average cluster size M on the mean charge q_m induced on the triggered strip is shown on Fig. 7. These data were obtained for different TFE/IB/SF$_6$ gas mixtures with the "screened" panel and 50 kΩ/sq graphite coating resistivity. Two figures differ in the charge scale: It is logarithmic for Fig. 7–a and linear for Fig. 7–b. It is seen from these figures that the mean cluster size for the given average charge does not depend on the gas mixture used. Two slopes of nearly straight lines are evident from Fig. 7–b for M as a function of q_m reflecting apparently different values of the relative CT amplitudes for i=$\pm$1 strips and the others. The slope of the first line is about 1.0 pC^{-1} and of the second one — 0.06 pc^{-1}.

On Fig. 8 we compare the M vs q_m data for two mixtures (1% and 2% of SF$_6$) obtained for the "screened" panel with the data for 95/3/2 and 98/0/2 mixtures, measured with the "ordinary" panel. For the both data sets, the graphite coating had low resistivity. No significant difference is seen for the two data sets. Thus, the efficiency of the tiny screening strips in cluster size reduction seems to be questionable, in agreement with the CTs result.

In Fig. 9 we compare the M vs q_m–dependence for the binary mixture measured for two different surface resistivities of the anode graphite coatings. A visible difference for the most

5

important charge range from 1 pC to about 10 pC is evident: For the higher resistivity anode the average cluster size M is reduced by at least 1.

Comparison of the observed "charge — cluster size" correlation with the predictions based on the CT data requires accurate simulation taking into account all the experimental details. Now we can only say that the observed correlation is in a rough agreement with that expected from Fig. 5. Namely, our estimated charge threshold is $q_{thr} \simeq 0.1$ pC. Having $r_{10} \simeq 5\%$, we expect that for $q \leq q_{thr}/r_{10} \simeq 2$ pC in most of the events the cluster size will be m=1. Similarly, as $r_{20} \simeq 0.5\%$, we expect m=(2–3) for charges from 2 to about 25 pC. For the higher charges the cluster size can be as high as the total number of strips.

Such a comparison is presented in Fig. 10, where integral cluster size distributions are shown for the three charge intervals. These distributions show the fractions f_m of events with the cluster size $\geq$m. The data were obtained for the binary gas mixture at HV setting 500 V above the efficiency plateau knee, ordinary panel and high resistivity graphite coating. For charges ≤ 2 pC, 65% of events have m=1. For the second charge interval, 80% of events have m$\leq$3, and for the last interval all ten strips are fired in about one half of events (only 10 strips were equipped with amplifiers in the given run).

4. STUDY OF CTs FOR DIFFERENT "RPC" CONFIGURATIONS

The ISP method also provided us with additional information that is not connected directly to the real RPCs but is, to our mind, interesting and useful for understanding the CTs phenomena.

In Fig. 11 we sketch three set-ups studied: (a) — "open" configuration, that contains one strip panel under study and gas gap mock-up/ISP, not covered by the opposite panel or continuous screen, (b) — complete RPC model and (c) — the "semi–open" configuration, which is similar to the real RPC but the opposite panel is lifted by (6–7) mm upward, thus increasing distance D between two strip planes to about (12–13) mm, instead of 5.7 mm for the real RPC studied (see Fig. 2). As is shown the HV is supplied to the needle through graphite coating. In all the cases the needle was positioned on the reference strip axis.

In Fig. 12, typical distributions of relative CT amplitudes among the strips are shown. For the "open" configuration (Fig. 12–a) the signals on all the neighbour strips have opposite (relative to the reference strip) polarity; they are unipolar. It is worth noting that the sum of these opposite sign relative amplitudes is approximately equal in an absolute value to unity. Because all the signals have the same length, this observation indicates an equality of the total charge, induced on the surrounding strips, to the reference charge, in an absolute value.

For comparison, Fig. 12–b shows the relative amplitudes distribution in real RPC, already discussed above. Bipolar signals were observed as it was shown in Fig. 3.

When the opposite panel is lifted upward in the RPC mock-up (Fig. 11–c), the CT picture is similar to the one observed for the "open" geometry, that is the CT signals are also unipolar and of the opposite polarity with respect to a reference pulse. This is of course completely different from the real RPC case. Relative amplitudes of CT signals are in this case (Fig. 12–c) smaller than in the "open" configuration case.

In Fig. 13 the relative CT amplitudes are shown for two adjacent strips as a function of needle position across strips for the first case (compare with Fig. 5 for the real RPC). It is seen that for the "edge region" between strips, signals on both of them have already the same polarity.

6

Thus, basing on our ISP study we should stress that the peculiarities of the CT signals are strictly limited to the particular case of the RPC design.

5. DISCUSSION

According to the results presented above we can distinguish two different mechanisms of the CTs in our RPC. Our inference is mainly based on the observed waveforms of CTs signals as a function of discharge position.

In the first mechanism the CT signals are the result of capacitive couplings between electrodes. For strips i=±1 adjacent to the triggered strip in the same panel, a suitable capacitance C_p is "strip–to–strip" capacitance. A signal created on the triggered strip is differentiated on C_p and acquires distinguished bipolar shape (Fig. 3–e,g). This is the mechanism that can be observed (and was studied at an early stage of our work) by applying an external voltage pulse to the reference strip and observing CTs signals on adjacent strips. For more distant strips |i|≥2, the mechanism of CTs is the same in nature but essential quantities are the (positive) signal created on the opposite orthogonal strip and C_p is in this case "panel–to–panel" capacitance (Fig. 3–f,h). Relative CTs amplitudes for this mechanism are determined to the first approximation by the ratios $C_p/(C_p+C_s)$, where C_s is "strip–to–ground" capacitance.

The other mechanism of CTs (the induction effect) was observed for discharge positions in the region about ±5 mm between adjacent strips in the real RPC design. For this mechanism the source of CT signals are the moving charge carriers themselves. This movement induces pulses of similar shape on the both adjacent strips.

The picture of CTs caused by the induction effect in RPC depend, according to our results, on the ratio between strip width W and the distance $\tilde{D}$ between the internal anode surface of the gas gap and the opposite strip plane [3,7]. For the real RPC, this value is $\tilde{D}/W \simeq 0.15$. It seems most likely that the induction mechanism is also responsible for the results obtained for "open" and "semi–open" configurations. For "semi–open" configuration, $\tilde{D}/W \simeq 0.45$ and for the "open" one — $\tilde{D}/W = \infty$. To explain the observed peculiarities, detailed calculations in the framework of "weighting field" method [4,5] seem to be required.

Of course, both above sources of CTs are present at the same time and in any electrodes configuration and the question is only which of them prevails in the given conditions, in particular, the detector design and particle track position.

We did not observe a significant reduction in CTs for the "screened" panel. To be effective as a screen for the capacitive CTs source, a tiny strip should be grounded on the spot of discharge position. In other case it should be also considered as capacitively coupled to the ground through C_{ts}. The screening coefficient for adjacent strips R_1 is then about $\tilde{C}_p/(\tilde{C}_p+C_{ts})$, where $\tilde{C}_p$ is parasitic capacitance of the tiny strip to the neighbour sensitive strip. From a rough consideration one can predict that for our case $R_1 \geq 0.6$.

The method of screening strips was used in plastic streamer tubes [14]. The authors reported on the reduction of the relative amplitude of the pulse on adjacent strip by a factor of two as compared with not screened array. But in this detector the sensitive and screening strips were 6 and 4 mm wide, respectively. The effect of the CT reduction was achieved at the expense of accompanying decrease of the useful signal by a factor of two.

Our data on the resistive HV electrodes "transparency" are in accordance with those published in [8]. For safe operation the surface resistivity of the graphite coating ≥500 kΩ/sq is desirable.

CONCLUSION

Study of CTs arising for multi-strip read-out of RPC signals was carried out both in the beam exposures of the chamber and using the ISP method.

It was found that depending on the particle track co-ordinate across the triggered strip (± 15 mm with respect to the strip axis), the relative amplitude on adjacent strips varies between about 0.05 and 1 and for strips i=± 2 — from about 0.006 to 0.06. For other strips the observed relative amplitudes were of the order of 0.002–0.003.

No CTs and cluster size reduction was obtained for the "screened" panel with 1 mm wide screening strips between the sensitive ones as compared with the ordinary panel.

The surface resistivity of the graphite coating of the high voltage electrodes of the order of $\simeq 50$ kΩ/square was found to be insufficient: Very long pulses were observed on neighbour strips often having higher amplitudes than the prompt CT signals. For the surface resistivity of about 500 kΩ/sq, this effect is considerably suppressed. Accordingly mean cluster size is decreased by 1 in the most important region of mean charges from 1 to 10 pC.

The observed cluster size dependence on the charge induced on the triggered strip is in a rough agreement with expectations based on the CT results. For a more accurate comparison, detailed simulation of the experimental conditions is required.

Comparison of the obtained results with the existing predictions [6,7] is difficult because of a very specific character of the CTs peculiarities noted above. On the other hand, the results presented can be used as a guide to any calculations of the CTs which should reproduce, in their turn, the observed features.

ACKNOWLEDGEMENTS

References

[1] ATLAS Technical Design Report. Muon Spectrometer. — CERN/LHCC 97–22, Geneva, 1997.

[2] See, for example, J–P.Risher, R.L.Chase, IEEE Trans. on Nucl. Sci., Vol. NS–31, /num 1, 1984, 258; V.Bonvicini, M.Pindo, Nucl. Instr. Meth. Vol. A372, 1996, 93; W.R.Graves et al., Nucl. Instr. Meth., Vol. 176, 1980, 229.

[3] N.N.Fedyakin et al., Nucl. Instr. Meth.,Vol. A292, 1990, 445.

[4] V.Radeka, Ann. Rev. Nucl. Part. Sci., Vol. 38, 1988, 217.

[5] E.Gatti, G.Padovini, V.Radeka, Nucl. Instr. Meth., Vol. 193, 1982, 651.

[6] Th.Heubrandtner et al., Nucl. Instr. Meth., Vol. A419, 1998, 721.

[7] V.Ammosov, V.Korablev, R.Santonico, IHEP preprint 97–83, Protvino, 1997; submitted to NIM.

[8] G.Battistoni et al., Nucl. Instr. Meth., Vol. 202, 1982, 459.

[9] N.Fujivara et al., SLAC – PUB – 3063, 1983.

[10] C.Beard et al., Nucl. Instr. Meth., Vol. A286, Nos. 1,2, 1990, 117.

[11] S.M.Mari, IV International Workshop on RESISTIVE PLATE CHAMBERS AND RELATED DE-TECTORS, Scientifica Acta, Vol. XIII, № 2, 1998, p.331.

[12] I.Crotty et al., Nucl. Instr. Meth., Vol. A360, 1995, 514.

[13] V.Ammosov et al., ATLAS–COM–MUON–99–024, 23 August 1999.

[14] G. Battistoni et al., Nucl. Instr. Meth., Vol. 176, 1980, 297.
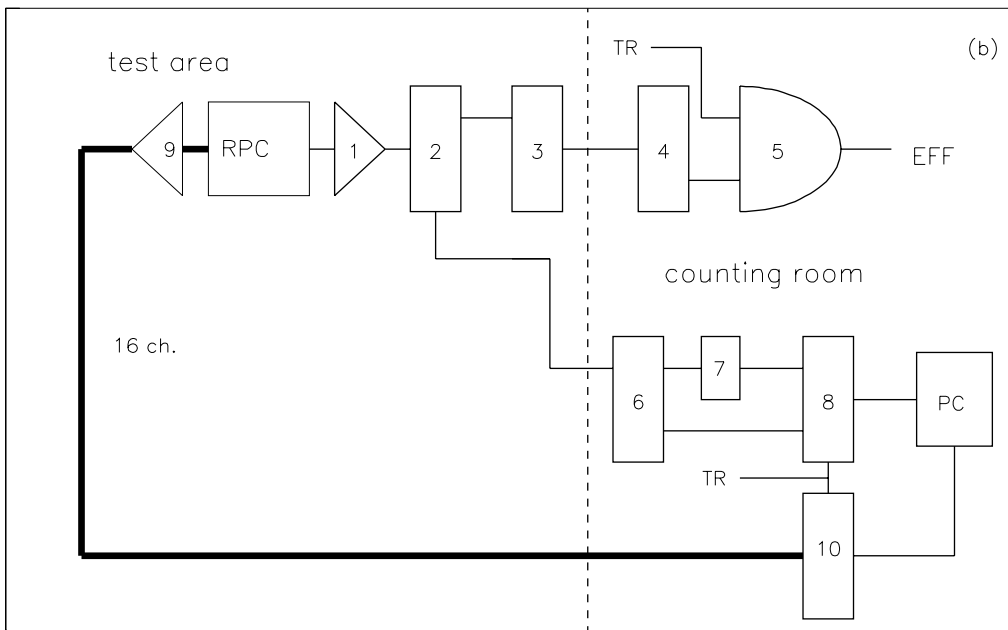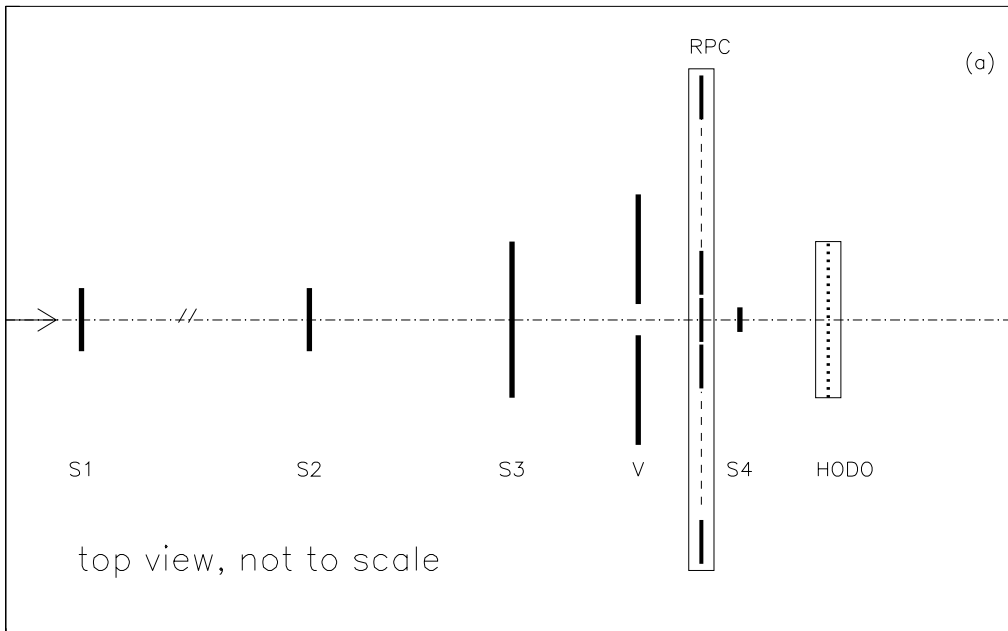
Fig. 1. Experimental set-up on the test beam: (a) — detectors lay-out, (b) — electronic circuits: 1 – amplifier 26 dB, 2 – fan-out, 3 – discriminator/shaper 6 mV, 4 – shaper 40 ns, 5 – coincidence unit, 6 – fan-out, 7 – attenuator 20 dB, 8 – QDC, 9 – 16 channel FE amplifier/discriminator, 10 – TDC.
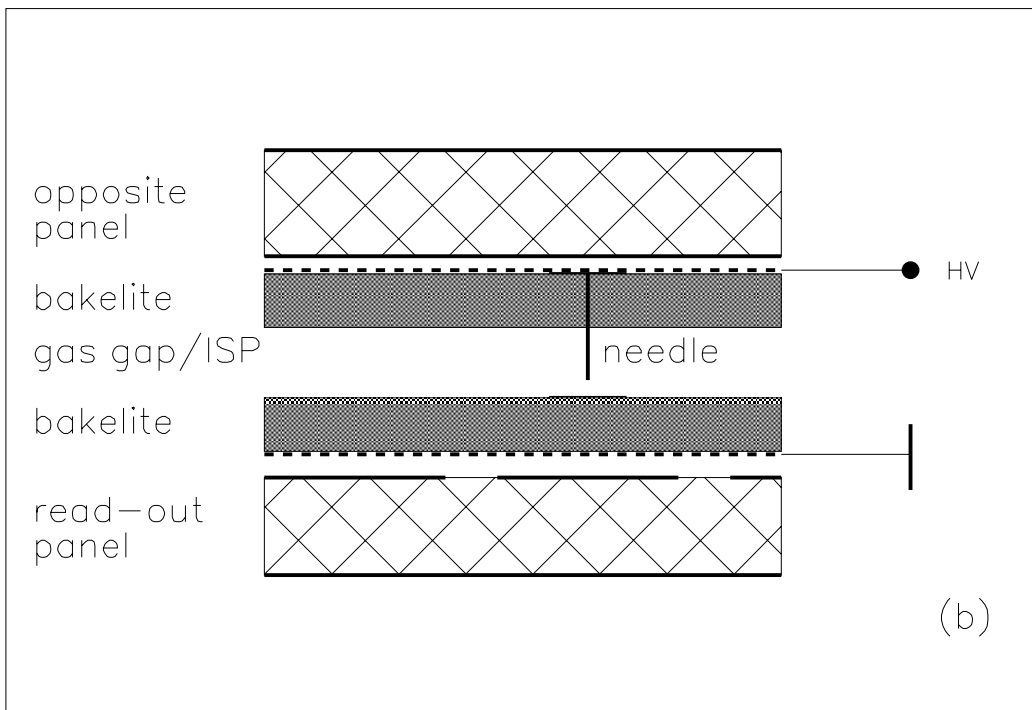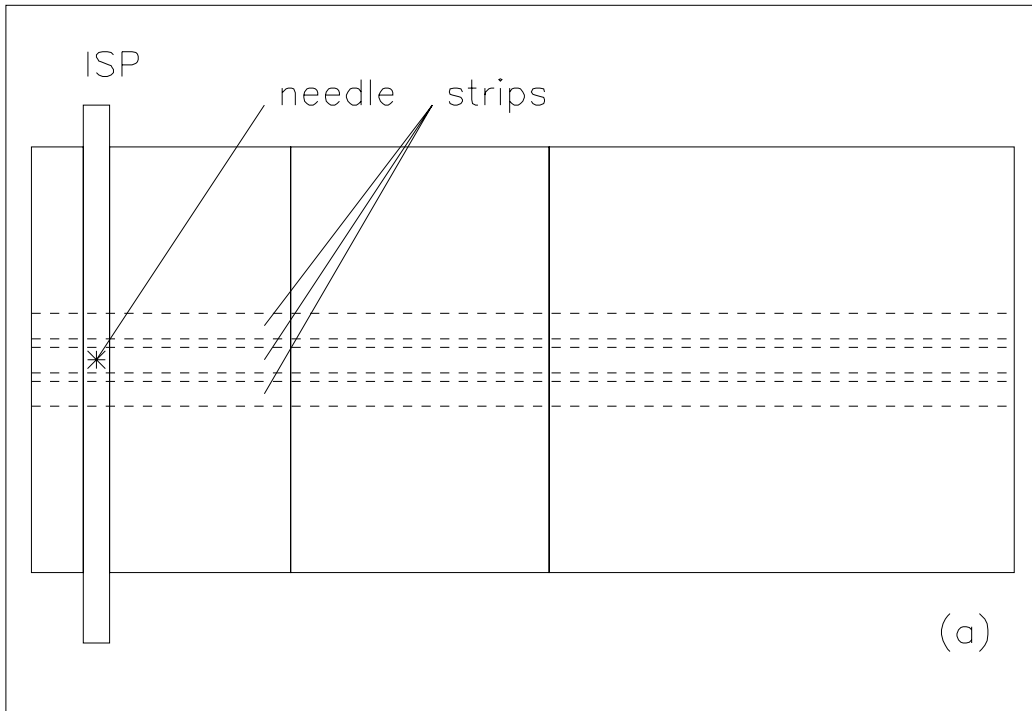
Fig. 2. Set-up for ISP studies: (a) — top view, not to scale, three strips are sketched by dashed lines; (b) — cross-sectional view.
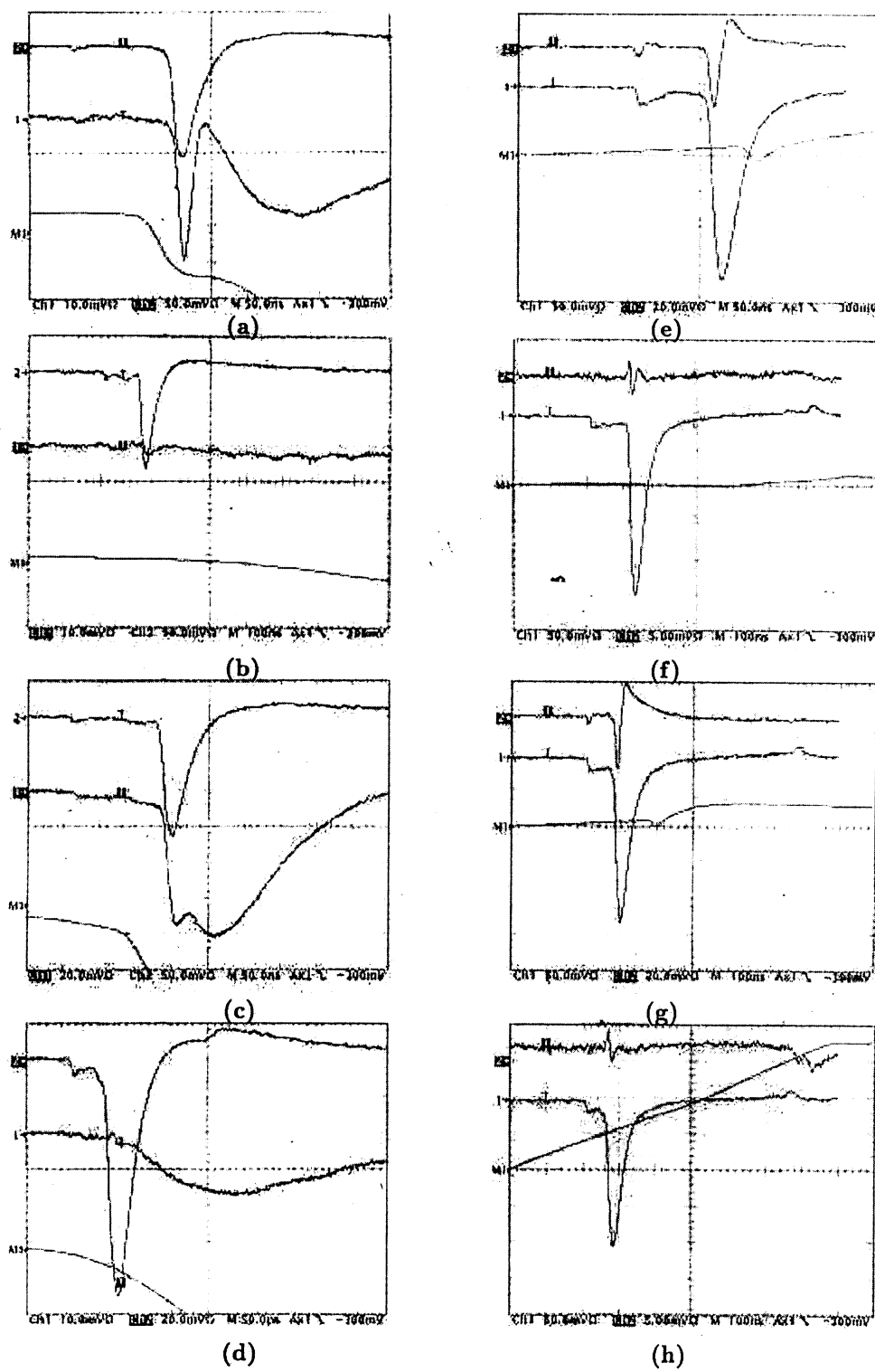
Fig. 3. Signal waveforms: (a–d) — low resistivity anode, Ch.2 — reference strip i=0, Ch.1 — i=−1(a), i=−2(b), i=+1(c), i=+2(d); (e–h) — high resistivity anode, Ch.1 — reference strip i=0, Ch.2 — i=−1(e), i=−2(f), i=+1(g), i=+2(h).

11
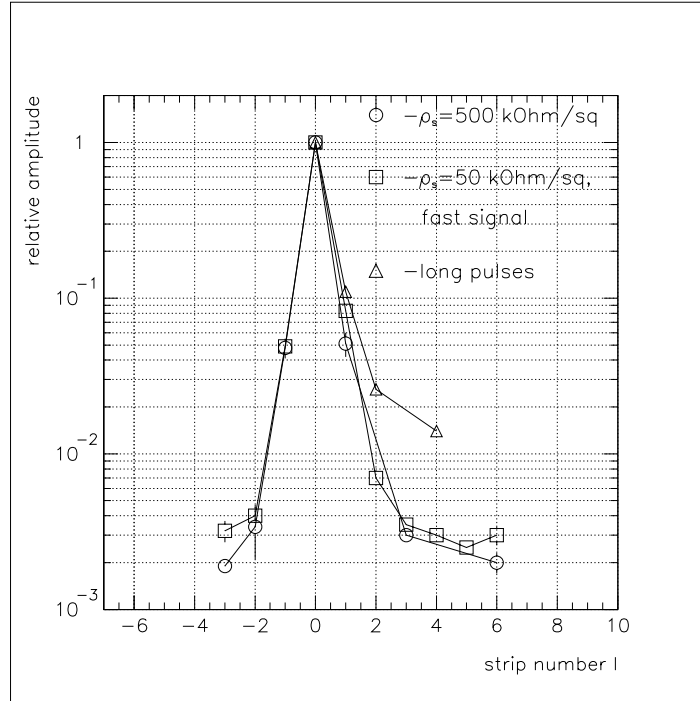
Fig. 4. Distribution of CT signals over strips for low and high graphite surface resistivities, beam data.
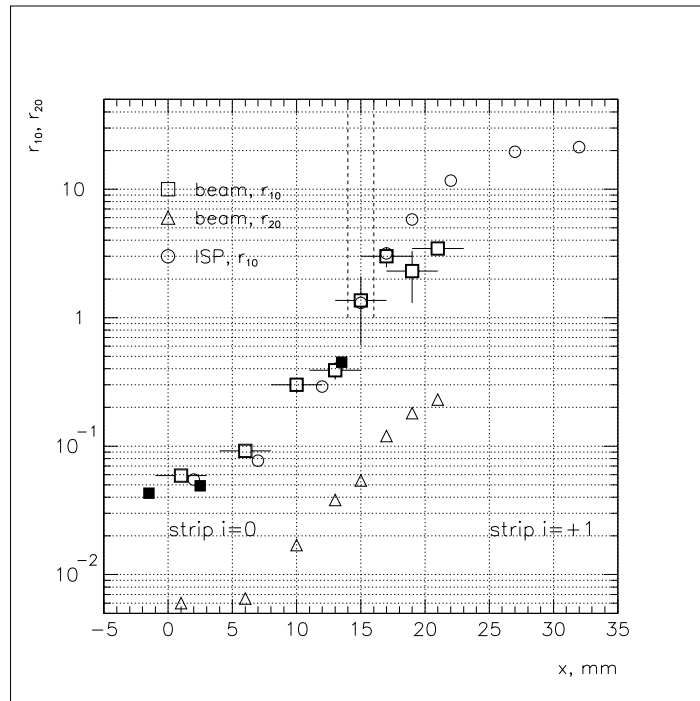
Fig. 5. CT dependence on the discharge position: ratios r_{10} and r_{20} as a function of the trigger or ISP needle positions. Open symbols — "anode" strips, solid — "cathode" strips.
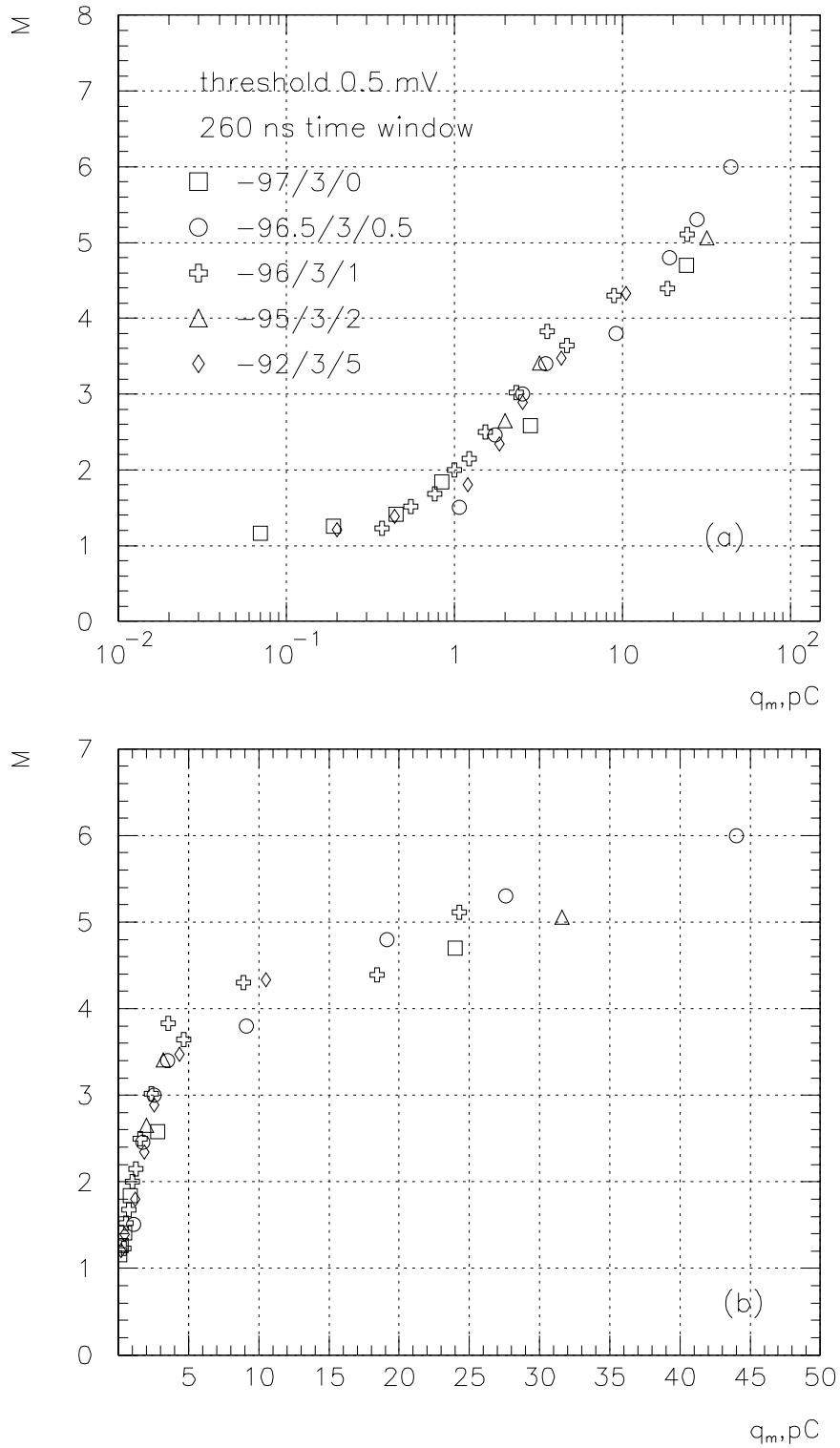
Fig. 7. Average cluster size M as a function of mean charge q_m for different TFE/isobutane/SF$_6$ mixtures. (a) — logarithmic charge scale, (b) — linear charge scale.

13
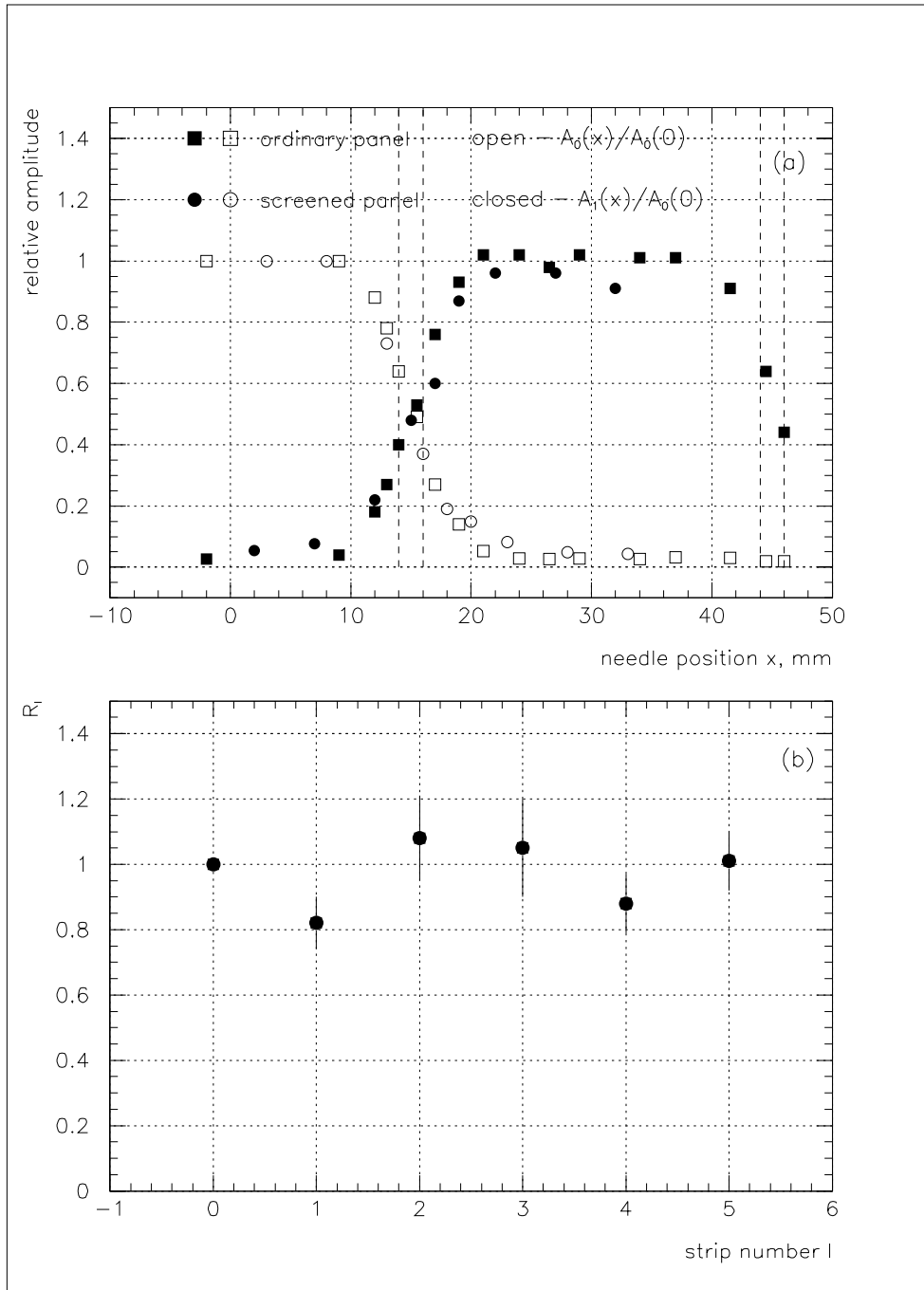
Fig. 6. Comparison of CTs for "screened" and "ordinary" strip panels: (a) — signal partition between adjacent strips for two panel designs; (b) — ratios of CTs relative amplitudes for "screened" and "ordinary" panels.

14
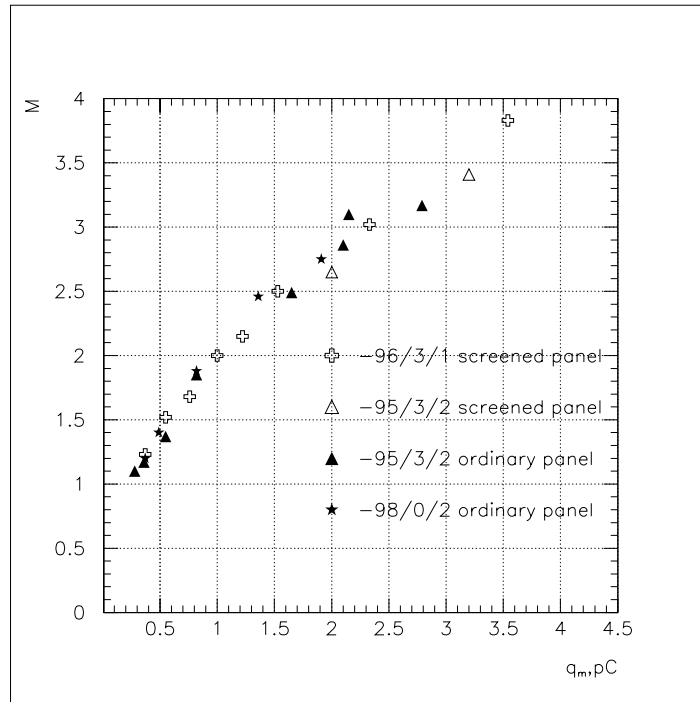
Fig. 8. Comparison of cluster sizes for screened and ordinary panels.
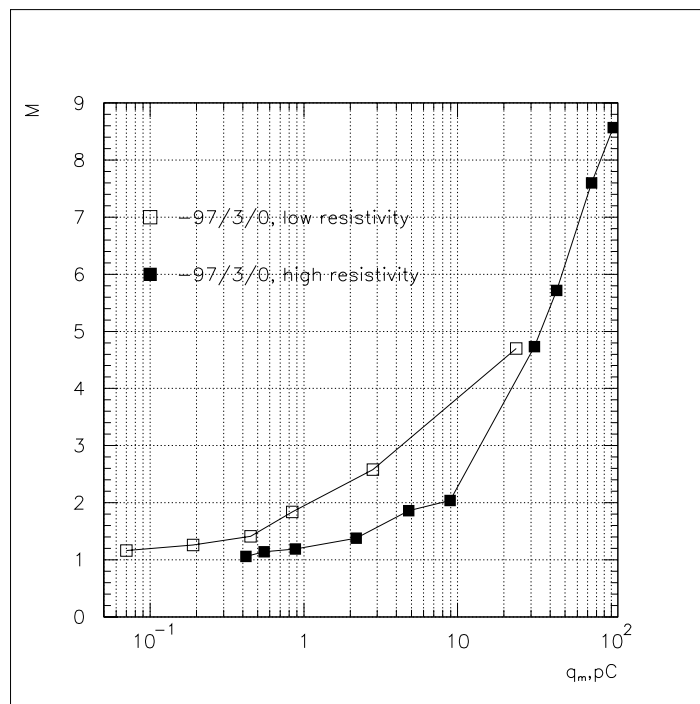
Fig. 9. Comparison of cluster sizes as a function of mean charge for two anode surface resistivities.

15
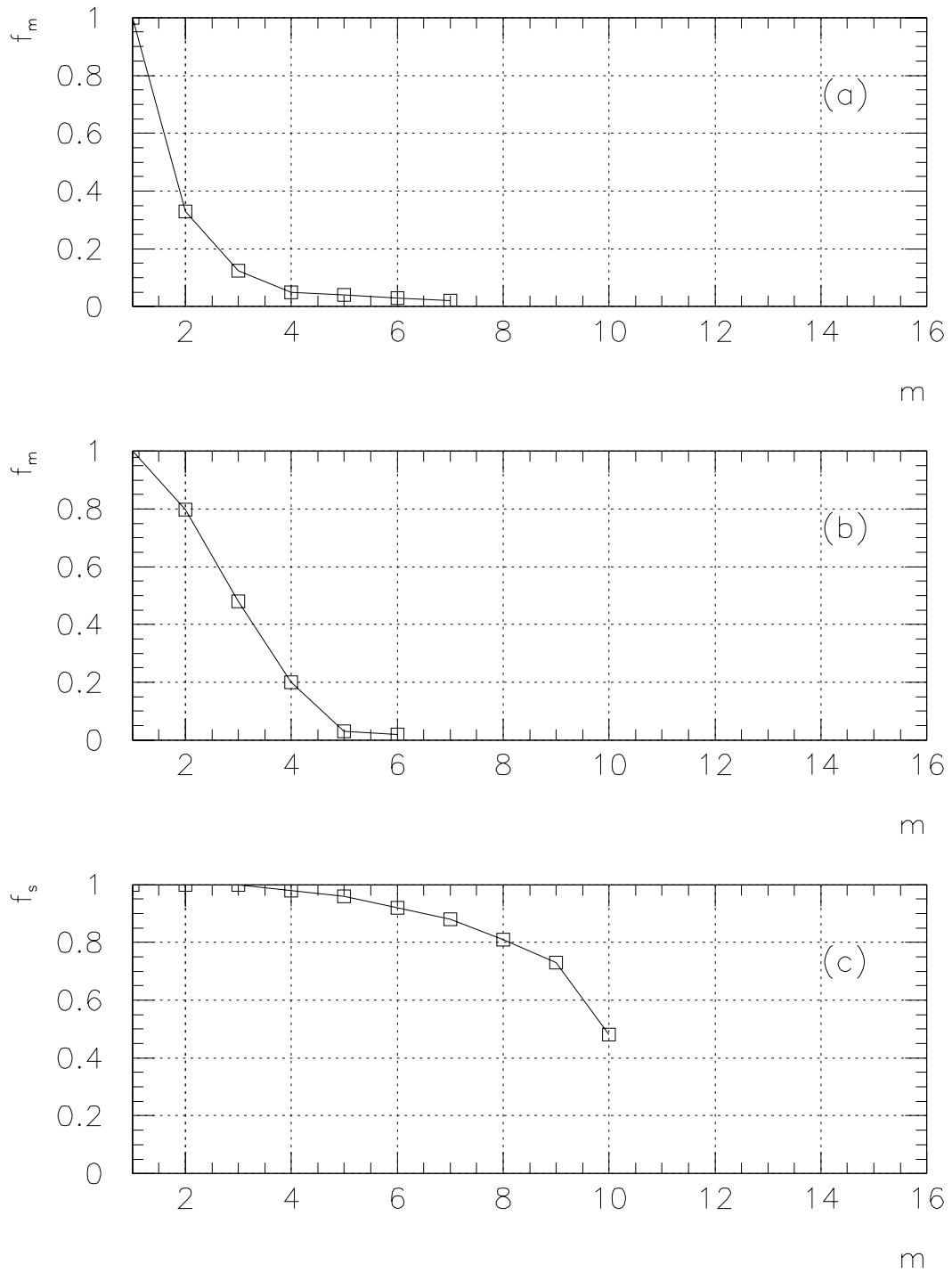
Fig. 10. Integral cluster size distributions for given charge intervals: (a) — 0≤q≤2 pC, (b) — 2≤q≤25 pC, (c) — 25≤q≤100 pC.
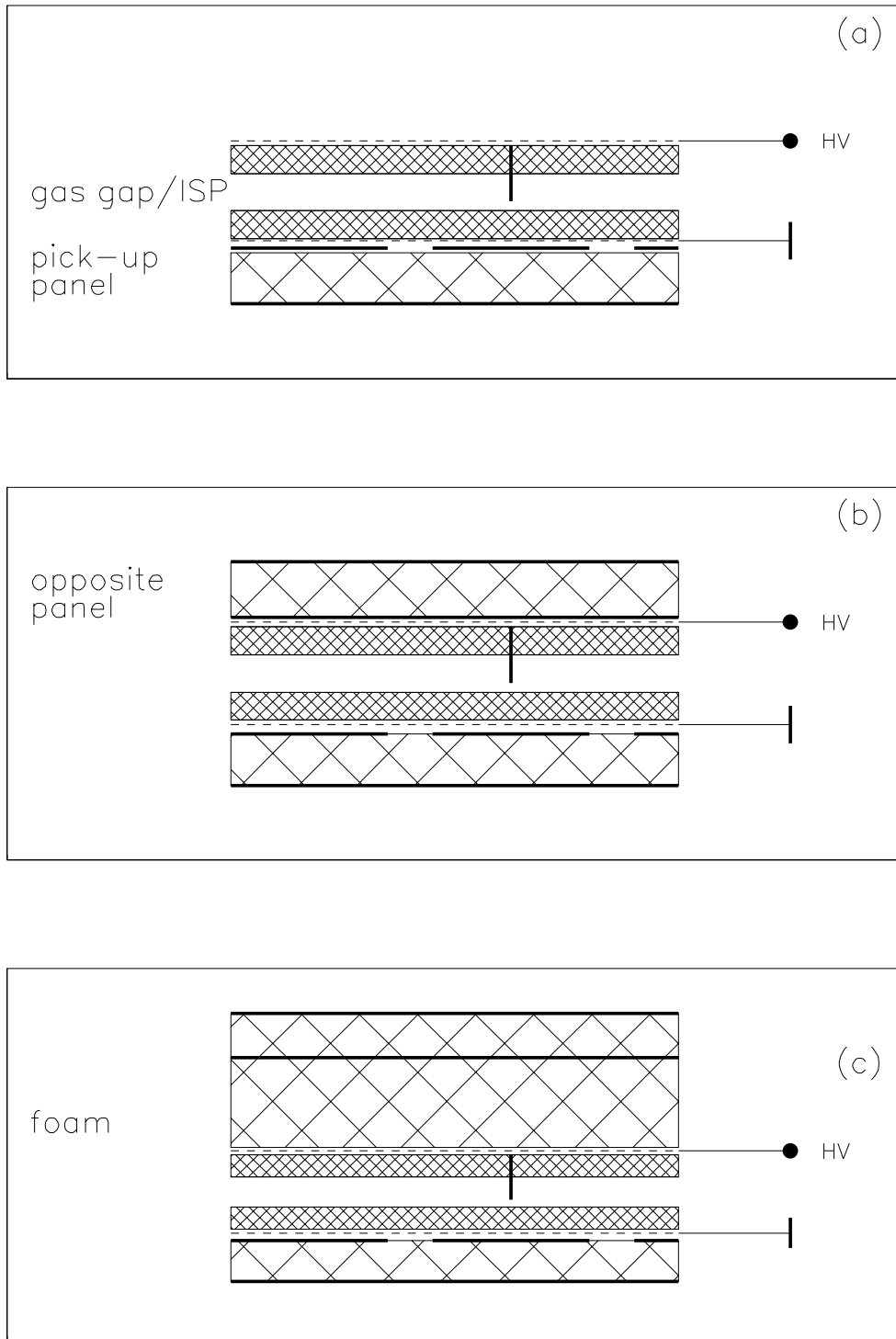
Fig. 11. Sketches of additional set-ups used in CT studies with ISP: (a) — "open" configuration, (b) — real RPC and (c) — "semi-open" configuration, opposite strip panel shifted 6 mm upward.
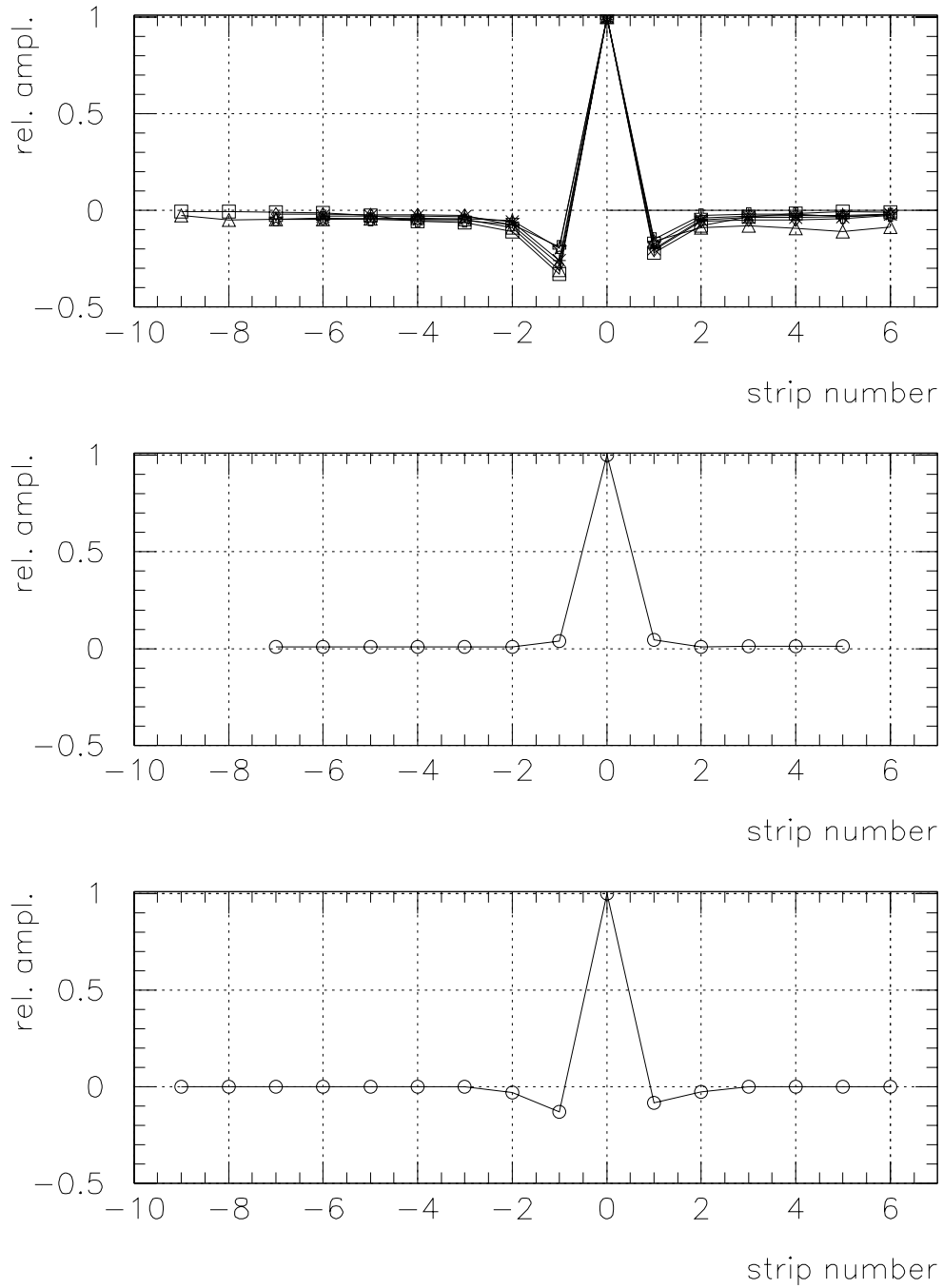
Fig. 12. Relative amplitudes distributions among strips for (a) — "open" configuration, (b) — real RPC and (c) — "semi-open" configuration.
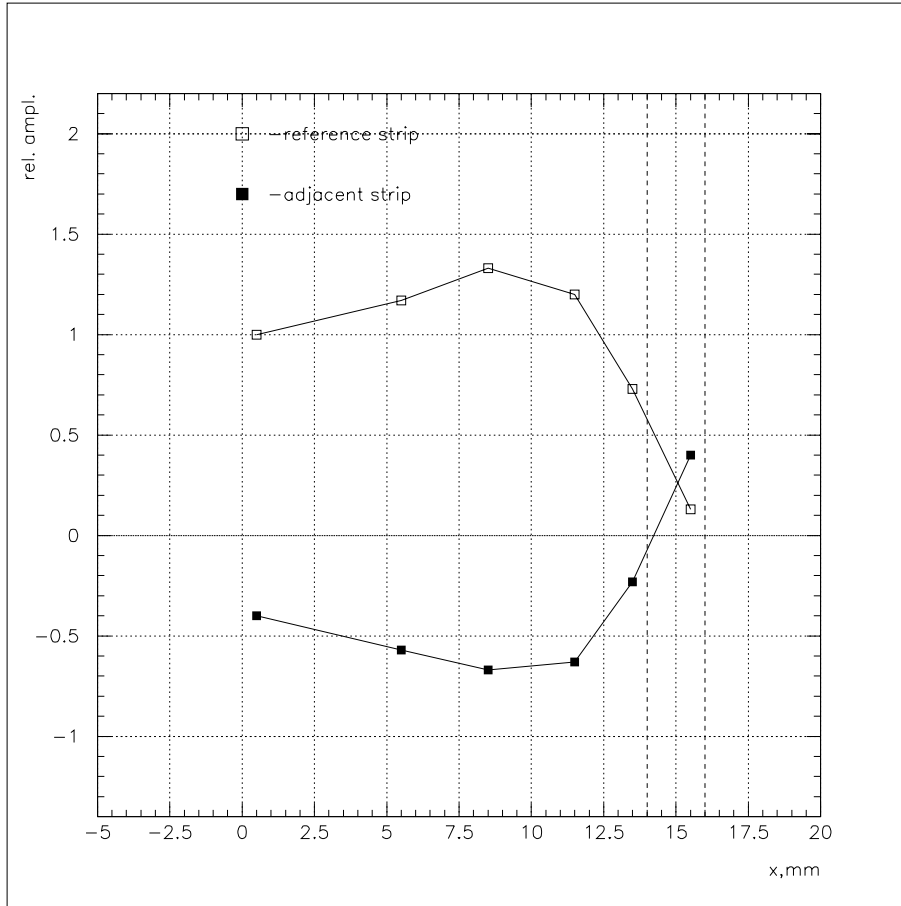
Fig. 13. Relative amplitudes for adjacent strips as a function of ISP needle position, "open" configuration.

В.В.Аммосов и др.

Многостриповое считывание в РПК: перекрестные наводки и размер кластера.